Determination of heavy metals in rice (Oryza sativa L.) and soil using AuNP/BiNP/MWCNT/Nafion modified glassy carbon electrode

Tim Aren O. Salinas [a], Michelle T. Natividad [a,b,*], Shirley T. Palisoc [a,b]

[a] *Condensed Matter Physics Laboratory, De La Salle University, Manila, 922, Philippines*
[b] *Condensed Matter Research Unit, CENSER, De La Salle University, 2401 Taft Avenue, Manila, 922, Philippines*

ARTICLE INFO

ABSTRACT

This paper presents the fabrication and application of a gold nanoparticle (AuNP)/bismuth nanoparticle (BiNP)/multi-walled carbon nanotubes (MWCNT)/Nafion-modified glassy carbon electrode for the determination of lead (Pb) and cadmium (Cd) via anodic stripping voltammetry (ASV). The ASV parameters as well as the AuNP and BiNP contents of the electrode modifier were optimized. The surface morphology, elemental composition, and electrochemical performance of the modified electrode were characterized using scanning electron microscopy (SEM), energy-dispersive x-ray spectroscopy (EDX), and cyclic voltammetry (CV), respectively. The SEM and EDX results showed that the modifiers were present on the electrode surface, while the CV curves show the remarkable stability of the modified electrode. The limit of detection of the fabricated electrode is 2.20 ppb for cadmium and 0.58 ppb for lead. Real sample analysis was performed using rice plant parts: husk, grain, stalk, leaf, root, and soil where the rice plant was planted. The fabricated electrode was able to detect trace concentrations of Pb and Cd in the said samples.

1. Introduction

Rice (Oryza sativa L.) is one of the most important staple food worldwide, particularly in the Philippines. According to the Philippine Statistics Authority, rice consumption in the Philippines amounts to 93.39 % of all reported households [1]. This heavy reliance on rice as the primary source of nutrition makes it an irreplaceable commodity and an essential aspect of the lives of Filipinos. The magnitude of rice plantations present not just in the Philippines but also in most of Asia makes rice susceptible to being contaminated by harmful substances, particularly heavy metals. An example of this is the presence of traces of heavy metals found in the soils of small rice plantations near small-scale mining sites [2]. These areas' residents are at risk due to prolonged heavy metal exposure and contaminated food consumption. Aside from these small plantations, bigger plantations are also affected by the mining operations in the area, with as many as four different rice fields being contaminated during heavy rainfalls [3].

Heavy metals, specifically lead, cadmium, and mercury, are hazardous pollutants that adversely affect living organisms. Heavy metal poisoning, for instance, is a common sickness attributed to prolonged exposure or accidental consumption of known heavy metals. Despite the harmful effects of these elements, it is undeniable that they have important applications in the fields of medicine, agriculture, and technology [4]. The irresponsible handling and disposal of these elements by different industries is the primary source

---

of contamination of the environment. This improper waste management is widely regarded as the leading cause of soil contamination by heavy metals, which are inevitably absorbed by plants and subsequently enter the food chain. The consumption of plants with even trace amounts of heavy metals can harm human health and lead to serious health problems [5–13].

Various methods have been used to accurately quantify the amount of trace heavy metals in food samples. Among these are atomic absorption spectroscopy (AAS) and inductively coupled plasma mass spectroscopy [14]. However, these methods are far too expensive and require bulky equipment. An attractive alternative to these methods is anodic stripping voltammetry (ASV), an electrochemical method that is low-cost, highly sensitive, and relatively easy to perform. This method relies solely on the material that composes the working electrode and is rather sensitive to experimental conditions requiring constant supervision to avoid imprecise and inaccurate data [15].

The working electrode typically employed in ASV is the glassy carbon electrode (GCE) due to its wide electrochemical window. Modification of the GCE surface is usually done to increase its sensitivity. In this study, gold nanoparticles (AuNP), bismuth nanoparticles (BiNP), and multi-walled carbon nanotubes (MWCNT) were used to modify GCEs. Gold nanoparticles have been known to have high conductivity and stability and have proven excellent in modifying electrodes [16]. Bismuth is usually used to modify electrodes due to its inexpensiveness and high sensitivity; it is also non-toxic and has a wider range of potential [17]. Multi-walled carbon nanotubes exhibit excellent suitability for the determination of heavy metals via ASV due to their electrochemically active sites [18].

This study focuses on the fabrication of a AuNP/BiNP/MWCNT/Nafion-modified glassy carbon electrode that is relatively sensitive, has good stability, and has a low limit of detection (LOD). The fabricated electrode was used in anodic stripping voltammetry for the simultaneous detection of lead (Pb) and cadmium (Cd) in rice and soil samples.

2. Methodology

2.1. Chemicals and reagents

Gold nanoparticles, cadmium chloride, and lead chloride were bought from Sigma-Aldrich (Singapore). The multi-walled carbon nanotubes and bismuth nanoparticles were obtained from Cheap Tubes Inc. (Cambridgeport, Vermont, USA) and Luoyang Tongrun Info Technology Co., Ltd. (Luoyang City, Henan, China), respectively. The Nafion solution was acquired from Fuel Cell Earth (Woburn, Massachusetts, USA).

2.2. Instruments

A PalmSens4 potentiostat (Palmsens BV, Houten, Netherlands) was used to perform the ASV and CV experiments. An ultrasonicator (Misonix, Inc., Farmingdale, New York, USA) was used to homogenize the casting solutions. The surface morphology and elemental composition analyses were performed using a JSM-5310 JEOL scanning electron microscope coupled with energy dispersive X-ray spectroscopy (JEOL USA Inc., Peabody, Massachusetts, USA). A ThermoLyne 48000 furnace was used to ash the real samples.

2.3. Preparation of the modified electrode

The GCE was washed with 10 ml of hydrochloric acid diluted with 20 ml of distilled water and was left to dry for 12 h to remove any dirt and impurities that may have adhered to the electrode surface. After the cleaning process, one end of the electrode was polished using sandpaper to smoothen the electrode surface. The electrode was then polished using a 0.3 μm then 0.05 μm alumina slurry against a glass slide until a somewhat glossy texture was obtained. The polished electrode was submerged in distilled water and was sonicated for 20 min. It was then submerged in ethanol and sonicated for 30 min. This was done to remove the alumina slurry and other foreign contaminants which may be present on the electrode surface. Afterward, the electrode was left to dry in air for 24 h at room temperature.

The casting solution was composed of MWCNT, AuNP, BiNP, and Nafion. The mass of MWCNT was held constant at 1.0 mg while AuNP and BiNP were varied from 1.0 mg to 3.0 mg. The Nafion solution (15 wt%) with a volume of 0.333 ml was diluted with 4.667 ml of ethanol. The mixture was drop-coated on the surface of the prepared GCE using a Transferpette® S micropipette and was left to dry in air for 12 h at room temperature.

2.4. Characterization of the modified electrode

The surface morphology and elemental composition of the modified electrodes were characterized using scanning electron microscopy (SEM) and energy dispersive x-ray spectroscopy (EDX). The electrochemical performance of the modified electrodes was studied using cyclic voltammetry (CV).

2.5. Voltammetry

A three-electrode system was utilized wherein the AuNP/BiNP/MWCNT/Nafion modified GCE served as the working electrode, Ag/AgCl as the counter electrode, and platinum wire as the reference electrode. The electrolyte solution composed of 100 mL deionized water and 0.58 g NaCl was sparged with nitrogen gas during runs.
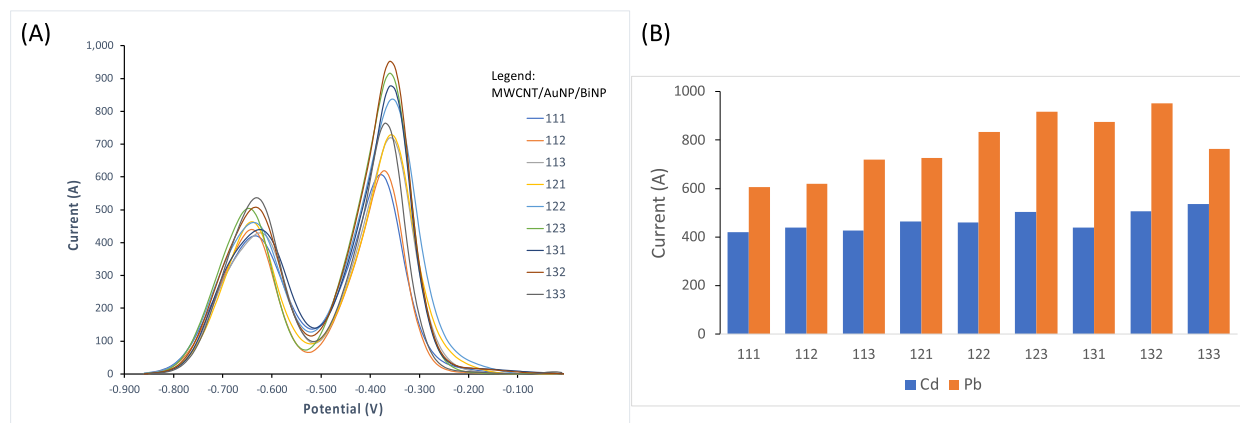
Fig. 1. (A) ASV curves and (B) histogram of anodic peak current for varying AuNP and BiNP contents of the electrode modifier.
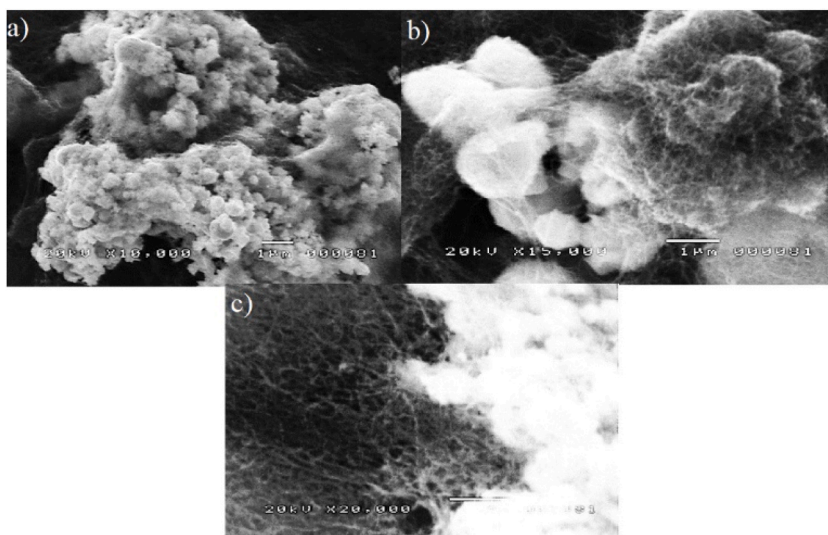
Fig. 2. SEM micrographs of the optimized electrode at (a) 10000x, (b) 15000x, and (c) 20000× magnification.

2.6. Real sampling

Real sampling was performed using rice plant parts, namely, grain, husk, stalk, leaves, roots, and soil samples where the rice was planted. The rice plant parts were cut, placed into different crucibles, and left under the sun to dry for 5–6 h to remove any remaining moisture. The dried samples were placed in a furnace at temperatures ranging from 600 °C to 650 °C for 17 h until the sample turned to white ash. The ashed sample was then digested with nitric acid at standard room temperature for 24 h and air-dried for 30 min. The powder obtained from the digestion was filtered and mixed with 200 ml of deionized water.

3. Results and discussion

3.1. Optimization of the modified electrode

The modified electrode was optimized by varying the masses of AuNP and BiNP at 1 mg, 2 mg, and 3 mg in the casting solution while the mass of MWCNT and the concentration of the Nafion solution were held constant. Subsequently, the electrodes obtained were employed as the working electrode in ASV for the simultaneous detection of 10 ppm each of Cd and Pb in the electrolyte solution. The scan rate, deposition potential, and deposition time were set at 0.1 V/s, −0.95 V, and 105 s, respectively.

The ASV curves obtained for the electrodes modified with varying AuNP and BiNP contents are shown in Fig. 1A. Fig. 1B shows the histogram of the anodic peak current for Cd and Pb. It can be seen in Fig. 1B that the electrode modified with 1 mg MWCNT, 3 mg AuNP, and 2 mg BiNP obtained the highest peak current for Pb and the second highest peak current for Cd. This was chosen as the optimized electrode.
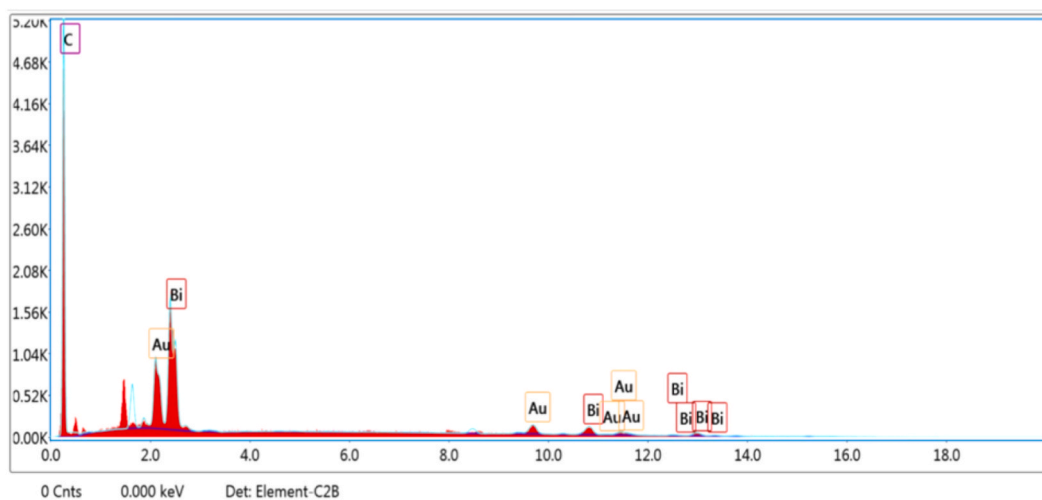
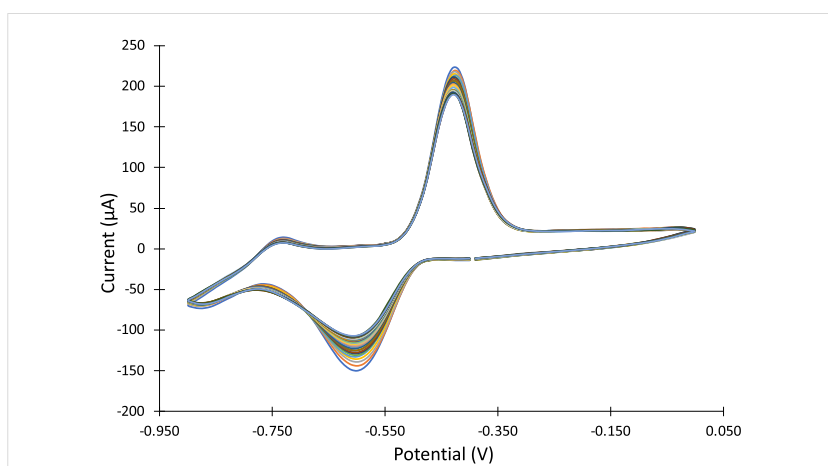**Fig. 3.** EDX spectrum of the optimized electrode.

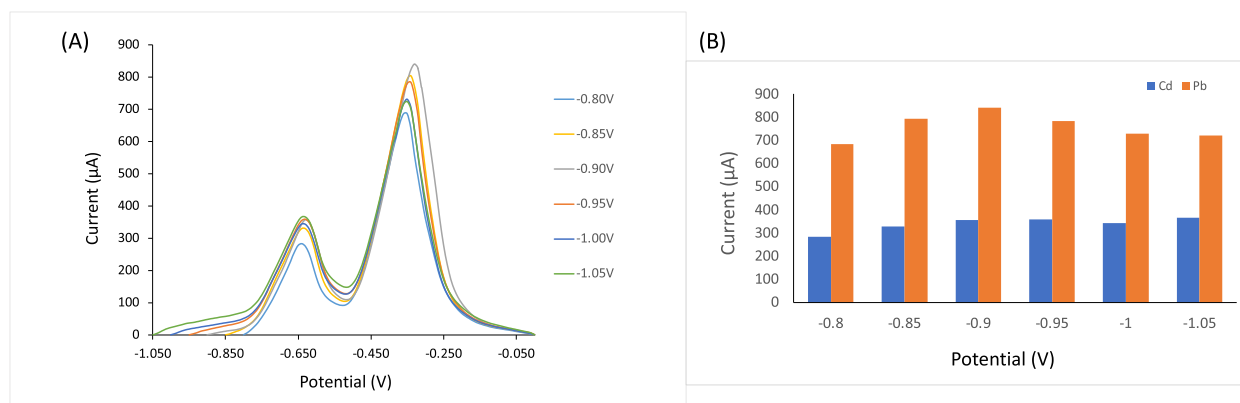**Fig. 4.** CV curves of the optimized electrode for 30 cycles.

Fig. 5. (A) ASV curves and (B) histogram of anodic peak current for varying initial potential.
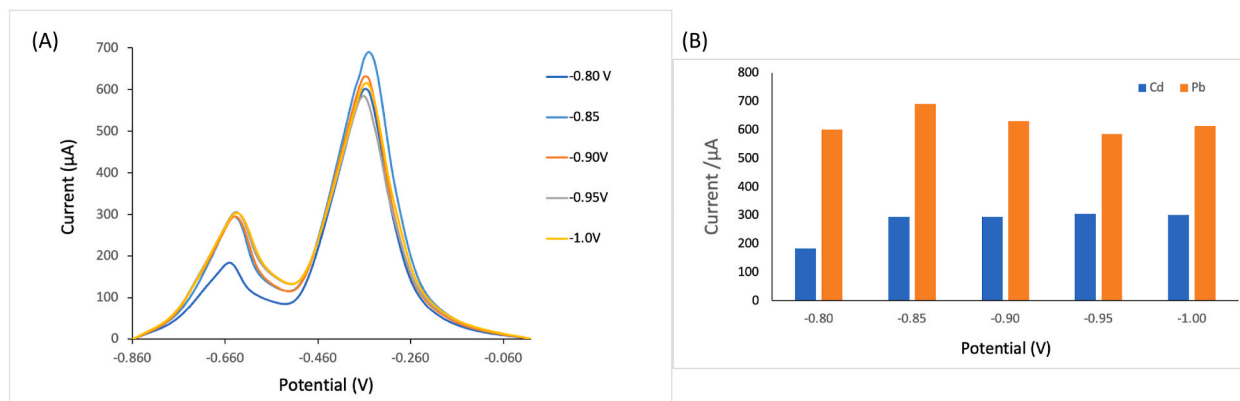
Fig. 6. (A) ASV curves and (B) histogram of anodic peak current for varying deposition potential.
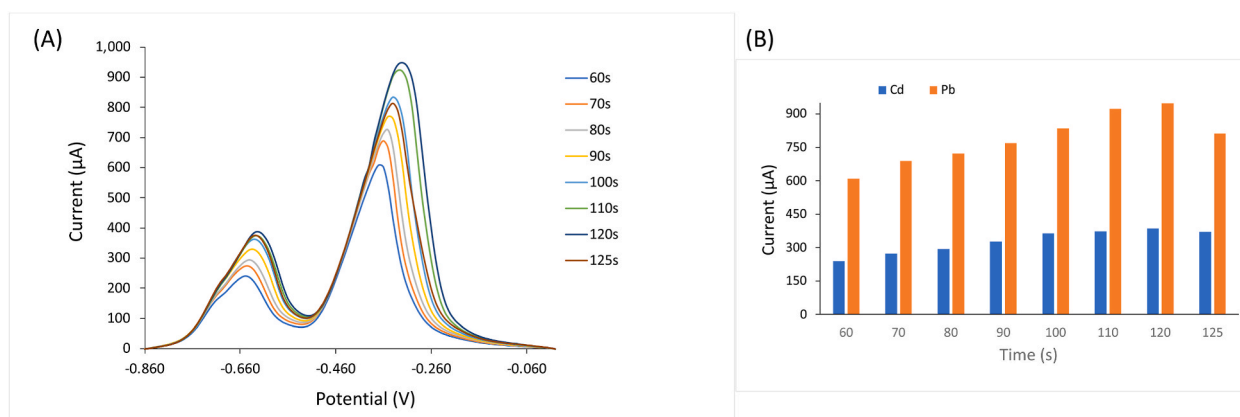

Fig. 7. (A) Voltammogram and (B) histogram of anodic current peaks for varying deposition time.

3.2. Characterization of the optimized electrode

The surface morphology of the optimized electrode was characterized using SEM. The micrographs of the optimized electrode at different magnifications are shown in Fig. 2(a–c). It can be observed from the micrographs that the AuNP, BiNP, and MWCNT (web-like structure) were successfully deposited on the electrode's surface. The EDX result also showed the presence of the nanoparticles on the surface of the electrode (Fig. 3).

The optimized electrode was characterized using cyclic voltammetry to determine its stability. Shown in Fig. 4 are the CV curves for 30 cycles. The modified electrode displayed remarkable stability with successive scans showing a mere 14.12 % variation between the first and last scans.

3.3. Optimization of ASV parameters

3.3.1. Initial potential

The initial potential was varied at increments of $-0.80V$, $-0.85V$, $-0.90V$, -0.95, $-1.0V$, and $-1.05V$. Meanwhile, the deposition time remained constant at 105 s, the rest period at 6s, and the scan rate at 0.1 V/s. Fig. 5A and B shows the ASV curves and histogram of the anodic peak current, respectively, for varying initial potential. Fig. 5B shows that reducing the initial potential from $-0.80V$ to $-0.9V$ led to an increase in the anodic peak current for both Cd and Pb. For initial potentials less than $-0.9V$, the anodic peak current decreased for Pb and stayed almost constant for Cd. Therefore, the optimal initial potential is $-0.90V$.

3.3.2. Deposition potential

The deposition potential was varied at increments of $-0.80V$, $-0.85V$, $-0.90V$, -0.95, $-1.0V$ while the deposition time remained constant at 105 s, the rest period at 60 s, the initial potential at $-0.85V$, and the scan rate at 0.1 V/s. Fig. 6A shows the ASV curves while Fig. 6B shows the histogram of the anodic peak current for varying deposition potential. It can be observed from Fig. 6B that for deposition potentials less than 0.85 V, the peaks started to level off. Therefore, the optimized deposition potential is -0.85 V.
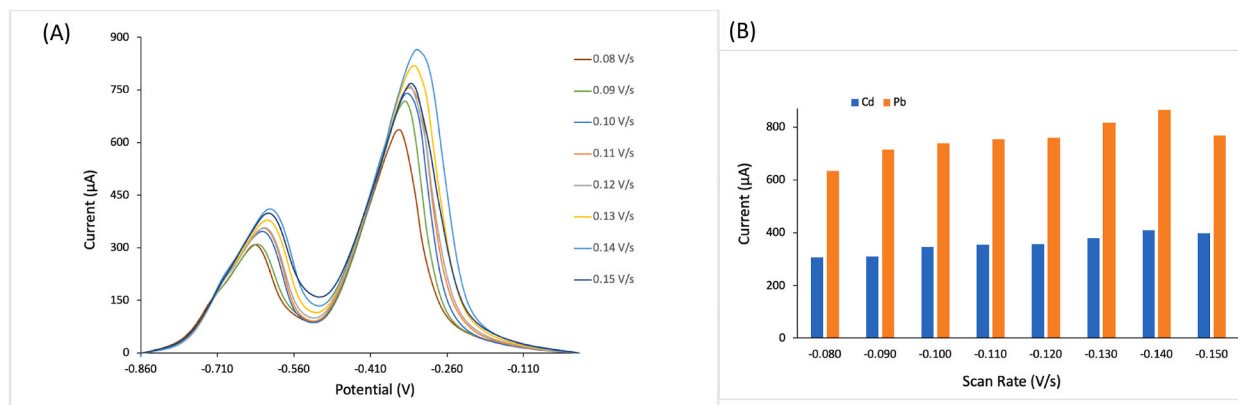
Fig. 8. (A) ASV curves and (B) histogram of anodic current peaks for varying scan rates.
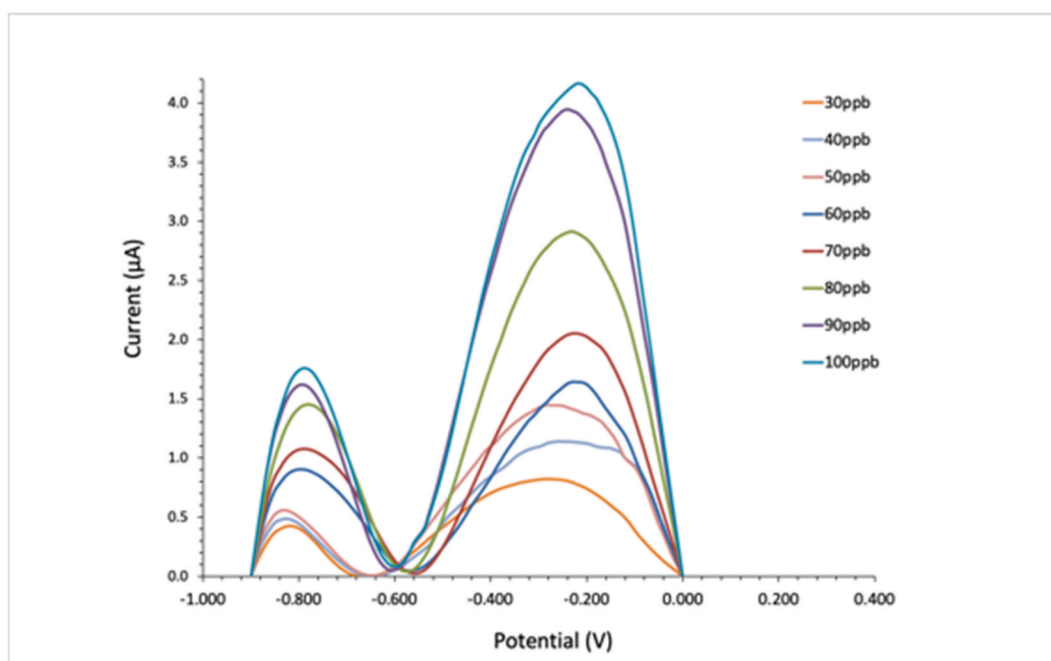

Fig. 9. ASV curves for varying concentrations of lead and cadmium.

3.3.3. Deposition time

The deposition time was varied from 60s to 125s while the deposition potential, rest period, initial potential, and scan rate were held constant at −0.95V, 60 s, −0.85V, and 0.1 V/s, respectively. The information depicted in Fig. 7 (A and B) reveals that increasing the deposition time from 60 s to 120 s resulted in an increase in the anodic peak current for both Cd and Pb, followed by a decrease at 125 s. Thus, the optimal deposition time is 120 s.

3.3.4. Scan rate

To determine the optimal scan rate, it was varied from 0.08 V/s to 0.15 V/s while the deposition time was held constant at 105 s, the deposition potential at −0.95 V, the rest period at 60 s, and the initial potential at −0.85V. Fig. 8 (A and B) demonstrates a rising pattern in the anodic peak current for Cd and Pb when the scan rate was increased from 0.08V/s to 0.14V/s. Subsequently, a decrease in the anodic current peak is observed upon further increase of the scan rate. Thus, 0.14V/s is the optimal scan rate.

3.4. Calibration curves

The ASV and calibration curves for varying concentrations of lead and cadmium using the optimized electrode are shown in Figs. 9 and 10 (A and B), respectively. The calibration curves were obtained by plotting the anodic peak current against the heavy metal
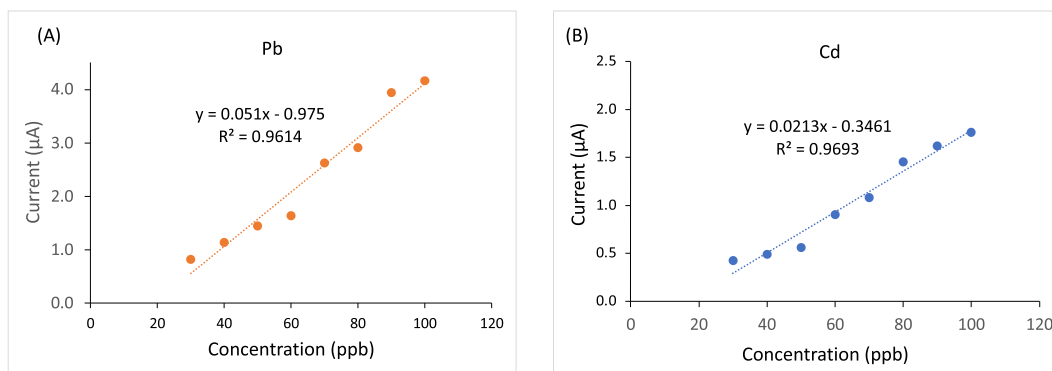
Fig. 10. Calibration curves for (A) lead and (B) cadmium. The limit of detection of the AuNP/BiNP/MWCNT/Nafion modified GCE is 2.20 ppb for cadmium and 0.58 ppb for lead.
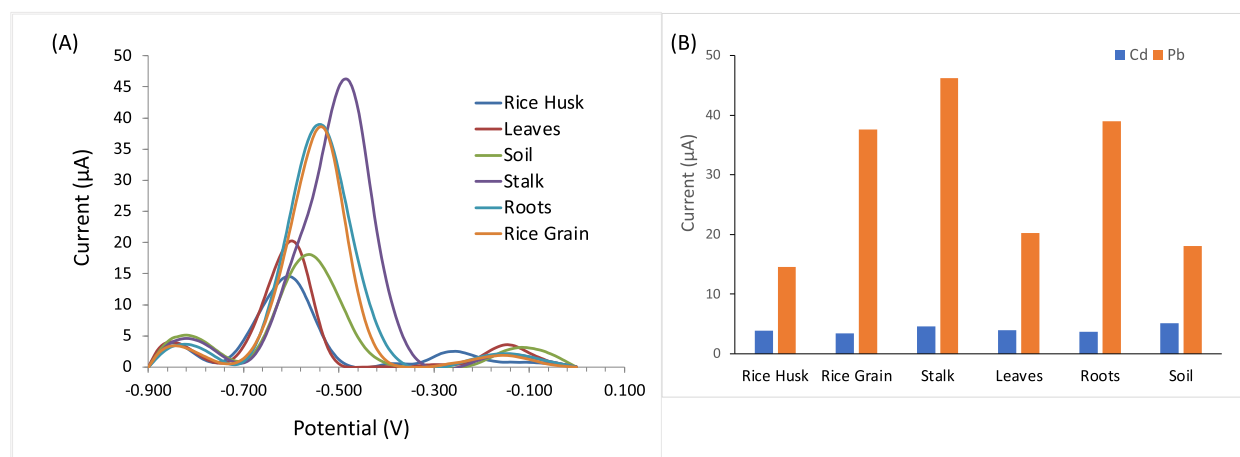
Fig. 11. (A) ASV curves and (B) histogram of anodic peak current for the real sample analysis.

Table 1
Cd and Pb content of the real samples.

Real Sample	Cd (ppb)	Pb (ppb)
Rice husk	199.10	304.7
Rice grain	176.49	775.26
leaves	204.75	415.85
stalk	233.01	925.12
roots	188.26	784.39
soil	258.92	374.38

concentration. The Pearson coefficients (0.96143 for Pb and 0.96810 for Cd) suggest a linear correlation between the anodic peak current and the concentration of the heavy metals.

3.5. Real sampling

The optimized electrode and optimal ASV parameters were utilized to assess the heavy metal content of the real samples. The ASV curves are shown in Fig. 11A, while Fig. 11B presents the histogram of the anodic peak current for Cd and Pb obtained for the rice plant parts and soil samples. Table 1 shows the measured Pb and Cd concentrations in the real samples. It can be observed from the figure and the table that all samples contained Cd and Pb. The rice stalk has the highest Pb content, and the soil has the highest Cd content. Aside from cadmium and lead, copper was also detected in the real samples.

4. Conclusion

The fabricated AuNP/BiNP/MWCNT/Nafion modified GCE was successful in detecting Cd and Pb in standard solutions and real samples. The optimal AuNP and BiNP contents of the electrode modifier were found to be 3 mg and 2 mg, respectively. The ASV parameters which obtained the highest current peaks are an initial potential of -0.9V, a deposition potential of -0.85V, a deposition time of 120 s, and a scan rate of 0.14V/s. Both the SEM and EDX results confirmed that the modifiers were successfully deposited onto the electrode surface. The CV curves showed that the fabricated electrode is stable. The calibration curves for both Pb and Cd displayed a strong linear correlation between the anodic peak current and heavy metal concentration in the range of 30 ppb–100 ppb. The LOD of the fabricated electrode is 2.20 ppb for cadmium and 0.58 ppb for lead.

Data availability statement

Data will be made available on request.

CRediT authorship contribution statement

Tim Aren O. Salinas: Data curation, Formal analysis, Investigation, Methodology, Writing – original draft. **Michelle T. Natividad:** Conceptualization, Formal analysis, Investigation, Methodology, Project administration, Supervision, Writing – review & editing. **Shirley T. Palisoc:** Conceptualization, Formal analysis, Funding acquisition, Investigation, Methodology, Project administration, Resources, Supervision, Writing – review & editing.

Declaration of competing interest

The authors declare that they have no known competing financial interests or personal relationships that could have appeared to influence the work reported in this paper.

References

[1] Philippine Statistics Authority, Consumption of Selected Agricultural Commodities in the Philippines, Volume 1, Philippine Statistics Authority, Philippines, Quezon City, 2017.
[2] O.D. Giron, J.E. Basa, K.S.E. Distor, K.G.N. Pusing, Mercury levels in Oryza Sativa cultivated in Philippine small-scale mining villages, Int. J. Environ. Stud. 74 (2016) 230–239.
[3] E. Abrahamsson, M. Ekelund, Human Exposure from Mercury in Rice in the Philippines, Uppsala University, Sweden, 2015, pp. 1–19.
[4] P.B. Tchounwou, C.G. Yedjou, A.K. Patlolla, D.J. Sutton, Heavy Metal toxicity and the environment, Exp. Suppl. 101 (2012) 133–164.
[5] J.J.V. Branca, G. Morucci, A. Pacini, Cadmium-induced neurotoxicity: still much ado, Neural Regen. Res. 13 (11) (2018) 1879–1882.
[6] P. Lentini, L. Zanoli, A. Granata, S.S. Signorelli, P. Castellino, R. Dell'Aquila, Kidney and heavy metals - The role of environmental exposure (Review). Mol. Med. Rep 15 (2017) 3413–3419.
[7] E.K. Silbergeld, M. Waalkes, J.M. Rice, Lead as a carcinogen: experimental evidence and mechanisms of action, Am. J. Ind. Med. 38 (2000) 316–323.
[8] M.R. Culen, R.D. Kayne, J.M. Robins, Endocrine and reproductive dysfunction in men associated with occupational inorganic lead intoxication, Arch. Environ. Health 39 (1984) 431–440.
[9] G. Assennato, C. Paci, M.E. Baser, R. Molinini, R.G. Candela, B.M. Altamura, R. Giorgino, Sperm count suppression without endocrine dysfunction in lead-exposed men, Arch. Environ. Health 42 (1987) 124–127.
[10] A. Bernard, Renal dysfunction induced by cadmium: biomarkers of critical effects, Biometals 17 (2004) 519–523.
[11] C.-L. Hsiao, K.-H. Wu, K.-S. Wan, Effects of environmental lead exposure on T-helper cell-specific cytokines in children, J. Immunotoxicol. 8 (2011) 284–287.
[12] K.R. Mahaffey, Nutritional factors in lead poisoning, Nutr. Rev. 39 (1981) 353–362.
[13] N.D. Vaziri, Mechanisms of lead-induced hypertension and cardiovascular disease, Am. J. Physiol. -Hear. Circ. Physiol 295 (2008) H454–H465.
[14] A. Helaluddin, R.S. Khalid, M. Alaama, S.A. Abbas, Main Analytical Techniques used for elemental analysis in various Matrices, Trop. J. Pharm. Res. 15 (2016) 427–434.
[15] D. Harvey, Chapter 11: Electrochemical Methods in Analytical Chemistry 2.1, DePauw University, Greencastle, Indiana, 2016.
[16] D. Lima, G.N. Calac, A.G. Viana, C.A. Pessôa, Porphyran-capped gold nanoparticles modified carbon paste electrode: a simple and efficient electrochemical sensor for the sensitive determination of 5-fluorouracil, Appl. Surf. Sci. 427 (2018) 742–753.
[17] S. Palisoc, M. Natividad, Y.A. Malabuyo, R.C. Pereja, Determination of heavy metals in root crops using bismuth nanoparticles modified graphene paste electrode, Agron. Res. 17 (2019) 245–260.
[18] S. Palisoc, M. Natividad, N. De Jesus, J. Carlos, Highly sensitive AgNP/MWCNT/Nafion modified GCE-Based sensor for the determination of heavy metals in Organic and non-organic Vegetables, Sci. Rep. 8 (2018) 1–13.